ELSEVIER

Polymer 44 (2003) 729–741

polymer

www.elsevier.com/locate/polymer

Interdiffusion and phase behavior at homopolymer/random copolymer interfaces

Erin L. Jablonski, Russell E. Gorga, Balaji Narasimhan*

Department of Chemical Engineering, Iowa State University, 2035 Sweeney Hall, Ames, IA 50011-2230, USA

Received 22 July 2002; received in revised form 22 October 2002; accepted 25 October 2002

Abstract

Interdiffusion in polymer bilayers of polystyrene (PS) and the statistically random copolymer poly(styrene-*r*-4-bromostyrene) (PBS), $(C_8H_{(8-x)}Br_x)_N$, where x is the mole fraction of brominated repeat units in the copolymer and N the degree of polymerization, was studied using Rutherford backscattering spectroscopy (RBS). PS/PBS bilayers with $0.04 < x < 0.63$ and the ratio N_{PS}/N_{PBS} varied from $0.06 < N_{PS}/N_{PBS} < 18.1$ were examined. PBS volume fraction versus depth profiles were obtained from the evolution of the bromine peak in the RBS spectra. It is shown that as the phase boundary is approached, interdiffusion occurs until layer compositions indicative of binodal conditions are reached. These observations are in very good agreement with phase diagrams obtained using Flory–Huggins theory and a PS/PBS interaction parameter measured using small angle X-ray scattering. For $N_{PS}/N_{PBS} \neq 1$, the mobility is dictated by the faster diffusing (lower N) component, resulting in an interface which moves toward the faster diffusing component. This result is consistent with fast mode theory; equilibrium conditions correspond to the asymmetry of the phase diagrams. Mutual diffusion coefficients were determined by comparison of the RBS data to a mean-field interdiffusion model using the fast mode expression for mobility. The mutual diffusion coefficient is shown to decrease with increasing N and x and increase with temperature. The implications of this miscibility dependence of the interdiffusion behavior, based on both composition of the copolymer and degree of polymerization, are discussed in the context of strengthening homopolymer/random copolymer interfaces.

Keywords: Interdiffusion; Phase behavior; Miscibility

1. Introduction

Composite polymeric materials tailored to possess properties of strength, elasticity, and adhesion are considerably affected by their interfacial characteristics. A detailed understanding of interfacial molecular phenomena and the parameters controlling the driving force for interdiffusion in polymer systems can have significant impact on the design of such materials. Applications include injection molding, compatibilizer/blend technology, co-extrusion, adhesives, electronic materials, and high performance nano-composites [1]. Overall, our work aims to identify molecular properties that influence interface performance and obtain meaningful relationships between molecular properties (interdiffusion, interfacial width, interaction parameter, phase behavior, and blend morphology) and macroscopic properties (interfacial fracture energy).

The evolution of the interface when two polymers are brought into contact above T_g has been studied extensively through experiments and models [1–13]. Many polymer/polymer interfaces (and blends) are partially miscible, i.e. they have a Flory–Huggins interaction parameter, χ, near the spinodal interaction parameter, χ_s. This work explores the effect of miscibility on interdiffusion in partially miscible bilayers of polystyrene (PS) and the statistically random copolymer poly(styrene-*r*-4-bromostyrene) (PBS), $(C_8H_{(8-x)}Br_x)_N$, where x is the mole fraction of brominated repeat units in the copolymer and N is the degree of polymerization. There has been much research using the partially miscible system of PS/PBS (or similar systems) and is discussed here for its relevance to this work. The PS/PBS system has been shown to exhibit an upper critical solution temperature (UCST) [14]. Bruder and Brenn [4] have investigated interdiffusion at deuterated polystyrene

* Corresponding author. Tel.: +1-515-294-8019; fax: +1-515-294-2689.
E-mail address: nbalaji@iastate.edu (B. Narasimhan).

0032-3861/03/$ - see front matter © 2002 Elsevier Science Ltd. All rights reserved.
PII: S0032-3861(02)00826-1

(d-PS)/PBS interfaces in the two-phase region of the phase diagram using elastic recoil detection (ERD) and found that the equilibrium composition of the interface represented the binodal concentrations for that system; from this work the Flory–Huggins interaction parameter was calculated and compared to the value obtained from small angle X-ray scattering (SAXS) measurements on similar systems [4,15]. In addition, interdiffusion coefficients were calculated from concentration profiles for similar systems. Stamm and co-workers [12,16,17] have used d-PS/PBS for interfacial width studies (using neutron reflectivity) and PS/PBS for fracture studies and shown the presence of various regimes in which the interfacial width is correlated to the fracture energy. The quantitative relationship obtained in that work is instructive, but limited because d-PS/PS has a small but positive χ due to the isotope effect [18]. To vary miscibility in the system, PBS copolymers with different extents of bromination were used. Green and Kramer [8,19,20] have used the d-PS/PS system to perform a comprehensive study of the self-diffusion coefficient of PS and shown the effects of temperature and molecular weight in these systems. SAXS has been used to measure the interaction parameter, χ, of the PS/PBS system and a weak dependence on blend composition has been observed [21]. Rafailovich and co-workers [11] have used both neutron and X-ray reflectivity to measure interface formation in the d-PS/PBS system to establish agreement between the methods. Other researchers have used this partially miscible system to study phase behavior and spinodal decomposition [22–24]. In addition, Green and Doyle [19,20] and Klein and co-workers [25,26] have used PS/d-PS systems and reported on the effects of thermodynamic slowing down, i.e. the slowing of diffusion as the system approaches the phase boundary due to thermodynamic limitations (immiscibility).

In order to describe interdiffusion in systems where there are chemically dissimilar species and/or a difference in molecular weight across the interface, theories have been developed which take into account the molecular weight dependence of mobility as well as the interactions between the constituents across the interface. The fast and slow mode theories of interdiffusion were independently developed in an effort to elucidate the molecular weight dependence of the mutual diffusion coefficient, specifically the mechanism of interdiffusion when the polymers have very different mobility. Brochard-Wyart [27] and co-workers derived the slow mode theory for interdiffusion using the chemical potential as the driving force for interdiffusion (based on previous work by de Gennes in 1981 [28]) and assuming equal but opposite fluxes of the interdiffusing components and composition-independent monomer–monomer friction coefficients. The slow mode theory predicts that interdiffusion is dominated by the slower diffusing species [29]. The fast mode theory developed by Kramer and co-workers [30] predicts that, as interdiffusion proceeds, the interface in a system with polymers of different molecular weight moves toward the lower molecular weight polymer. Assuming that unequal fluxes of species A and B are balanced by a net flux of vacancies across the interface, fast mode theory describes interdiffusion dominated by the faster diffusing polymer. Most research, both experimental and computational, supports the validity of fast mode theory [31–36]. Akcasu [31–33] has pointed out that there may be a 'cooperative component' to the kinetic term of the mutual diffusion coefficient, and that this cooperation will represent the movement of the chains relative to each other due to interactions. The theory proposed by Akcasu takes into account variable compressibility across the interface, thereby bridging the gap between the fast and slow mode theories.

Jabbari and Peppas [35] have developed a model to describe interdiffusion at interfaces of polymers with dissimilar physical properties. The model system comprises one fast moving component (high mobility) and one slow moving component (low mobility). The approach assumes that vacancies make up only a small fraction of the overall concentration and therefore do not substantially affect the free energy of mixing. A chemical potential gradient exists across an interface for polymers with different chemical structure and molecular weight; this chemical potential gradient is assumed to be the driving force for interdiffusion and only one-dimensional flux perpendicular to the interface is allowed [37]. Using the Flory–Huggins equation to relate chemical potential to the free energy of mixing of the two polymers and estimating values of the Onsager and friction coefficients and the blend zero-shear viscosity, they propose the following:

$$D_{\mathrm{M}} = \left(\frac{RTN_{\mathrm{b}}^{\mathrm{e}}}{f_{\mathrm{b}}^{\mathrm{m}}}\right)\left(\frac{1-\phi_{\mathrm{s}}}{N_{\mathrm{s}}} + \frac{\phi_{\mathrm{s}}}{N_{\mathrm{f}}}\right) \times \left(\frac{1-\phi_{\mathrm{s}}}{N_{\mathrm{s}}} + \frac{\phi_{\mathrm{s}}}{N_{\mathrm{f}}} - 2N\chi_{\mathrm{sf}}\phi_{\mathrm{s}}(1-\phi_{\mathrm{s}})\right) \quad (1)$$

Here, R is the gas constant; T, temperature; $N_{\mathrm{b}}^{\mathrm{e}}$ is the average number of repeat units between entanglements for the blend; $f_{\mathrm{b}}^{\mathrm{m}}$ is the blend monomeric friction coefficient; ϕ_{s} is the volume fraction of the slower moving component; N_{s} and N_{f} are the degrees of polymerization of the slow and fast components, respectively. From comparisons of this model to data for PS/PVME (polyvinyl-methyl-ether) system, they found the friction coefficient to be strongly composition dependent. They also report highly asymmetric diffusion profiles as further evidence of swelling of the slower moving component by the faster one, both above and below the glass transition of the slower diffusing component [38]. Further research in this group determined that, in the immiscible limit, miscibility effects, regardless of the respective mobility of each polymer, limit the extent of interdiffusion [9]. Other researchers have noted that asymmetric interdiffusion profiles will occur for strong concentration and temperature dependence of the molecular mobility [5].

With knowledge of what has been done by others, we discuss here the interdiffusion phenomena (and corresponding

phase behavior) for the PS/PBS system at various f, the volume fraction of brominated repeat units in the copolymer, and N, and demonstrate the correlation with phase behavior in this system. As mentioned before, the effect of miscibility on the interdiffusion in the homopolymer/random copolymer system PS/PBS is examined using Rutherford backscattering spectroscopy (RBS). The overall goal of this paper is to provide a basis to discern the nature of the thermodynamic (miscibility) and kinetic (mobility) effect on the interdiffusion behavior. Combinations of f and N designed to span a range of miscibility have been chosen; for given N_{PS} and N_{PBS}, system miscibility is controlled by f. Additionally, systems having the same f were studied for different values of the ratio N_{PS}/N_{PBS}. Phase diagrams for various extents of bromination and molecular weight have already been obtained and χ parameters have been measured using SAXS [39]. The PS/PBS systems, defined in terms of f, N_{PS}, and N_{PBS}, undergo phase transitions within the temperature range considered in this study [39]. In order to directly relate interdiffusion and phase behavior, identical polymers were used in the respective studies.

Table 1
Degree of polymerization, extent of bromination, and polydispersity of PS/PBS system

N	x	f	M_w/M
$(C_8H_{(8-x)}Br_x)_N$			
424	0	0	1.03
	0.07	0.08	
	0.20	0.22	
	0.25	0.28	
	0.42	0.46	
	0.63	0.66	
1370	0	0	1.03
	0.08	0.09	
	0.22	0.25	
	0.39	0.43	
	0.51	0.55	
4087	0	0	1.04
	0.25	0.28	
	0.43	0.47	
	0.59	0.63	
7670	0	0	1.05
7144	0.04	0.04	1.1
	0.20	0.22	
	0.48	0.52	

2. Experimental techniques

Monodisperse PS and PBS were obtained from Polymer Source, Inc (Dorval, Quebec). PBS was synthesized by the procedure described by Kambour and Bendler [22]. By controlling the amount of bromine added and the reaction time, PBS with varying extents of bromination was synthesized. ^{13}C NMR, elemental analysis, DSC, TGA, GPC, and UV–vis spectroscopy were used to characterize the polymer to ensure substitution of bromine in the *para*-position of the benzene ring and an unchanged degree of polymerization. Table 1 lists relevant properties of the polymers used in this study.

The bilayers are composed of a bottom layer of PS and a top layer of PBS. For the PS layer, a solution of PS in toluene was prepared and cast onto a pretreated silicon wafer using a spin coater (Headway Research, Garland, TX). The wafers were pretreated for 24 h in a solution of chromic/sulfuric acid to remove any organics and residual polishing silicones, and then cleaned by the RCA method [40]. The films were then dried at room temperature in a controlled atmosphere for 24 h followed by in vacuum at 25 °C for 6 h. Film thickness and surface roughness were measured by profilometry to yield relatively smooth (±3 nm) PS films of thickness 1–2 μm. For the PBS layer, a solution of PBS in toluene was prepared and cast onto glass slides using a spin coater, then dried in the same manner as the PS layers to yield thickness 0.3–1.5 μm. Film thickness was measured (on silicon) using an automated film thickness apparatus (Tencor, Mountain View, CA). The glass slides used for the PBS films were pretreated in a solution of chromic/sulfuric acid for 24 h, then for 10 min in each of the following: acetone, de-ionized water, 2-propanol, and toluene. The PBS films were floated off the slides onto de-ionized water. The corresponding PS film on the silicon wafer was used to pick up the floating PBS film to create the desired bilayer. The bilayer was then dried in a controlled atmosphere at room temperature for 24 h and in vacuum at 60 °C for 24 h. Samples were annealed at $\leq 10^{-3}$ Torr for appropriate times at various temperatures ($150 < T < 250$ °C), well above the glass transition temperature of both species [41], to allow interdiffusion. Both N-symmetric and N-asymmetric bilayers were prepared in this manner. We define N-symmetric bilayers as having $N_{PS}/N_{PBS} = 1$; N-asymmetric bilayers have $N_{PS}/N_{PBS} \neq 1$.

2.1. Rutherford backscattering spectroscopy

Rutherford backscattering spectroscopy (RBS) provides quantitative composition and depth information [42] with resolution at the interface (for our setup) in the order of 500 Å. The method to obtain concentration versus depth profiles from RBS spectra has previously been reported [5]. Kramer and co-workers [30] have successfully used RBS to study 'marker molecule' diffusion at polymer interfaces and to obtain concentration versus depth profiles in polymer systems where one of the species was preferentially stained with a heavy element [5]. However, interfaces in which chemically similar polymers are present on either side of the interface (as in this study) cannot be preferentially stained. For our studies, the bromine in the copolymer serves as a tag to follow the change in the composition of each layer with time.

The software used to analyze the RBS data was QUARK (QUantitative Analysis of Rutherford Kinematics) [43]. The input parameters include the type of ion used (He^{2+}), beam

energy, configuration (IBM or Cornell), detector angle, target angle, and solid angle. The adjustable parameters are charge on the sample, detector resolution, and dispersion (channel to energy conversion). Once these parameters are known the spectra are converted to energy versus depth profiles. The depth resolution of the technique used (RBS with slightly defocused beam) is estimated (using the detector resolution, dispersion, and stopping range of ions in matter [44]) to be 50 Å at the surface and approximately 500 Å at the interface (assuming an average interface at 8000 Å PBS + 100 Å gold overlayer).

Fig. 1(a) shows a typical RBS spectrum for an unannealed PS/PBS bilayer ($N = 7144$, $f = 0.04$) reported as normalized yield versus channel with a simulated fit. The simulations are constructed to estimate layer thickness and atomic compositions [45,46]. In this spectrum, the bromine peak corresponding to the PBS layer is clearly discernible. The corresponding concentration versus depth profile for the bromine peak is shown in Fig. 1(b). For the example considered in Fig. 1, the PBS layer is 3100 Å thick. It is instructive to note that the example shown in Fig. 1 corresponds to the lowest extent of bromination in our study. Since it is possible to detect bromine levels at $f = 0.04$, the bromine peak in the spectra for the greater extents of bromination are also detectable.

It has been reported that PBS is sensitive to radiation damage [4,5,15,47]. RBS spectra of PBS were observed to change appreciably and a depletion of bromine that increased towards the surface of the sample was detected; this depletion was attributed to loss of mobile HBr. A reported means of reducing this effect was to cool the sample [5,15,47,48]. In our work minimization of sample damage during analysis was achieved through gold-coating the sample to prevent charging and analyzing over a large annular region. Analyzing over this relatively large surface (ca. 200 mm^2) also allows for an averaging of heterogeneous effects whereas an intensely focused beam would impinge on the center of the sample with a total analysis surface of ca. 2 mm^2. To ensure that the above procedures minimized damage, spectra of the same sample were sequentially collected for multiple analysis times. Fig. 2 shows that there was no change observed in the spectra for times up to four times the typical analysis time. Another issue that was addressed is the appearance of contaminants in the sample spectra. Using an angle-resolved experiment [42,49], it was determined that the contaminants reside on the surface of the gold layer, and therefore do not interfere with interdiffusion at the PS/PBS interface. In some spectra a slightly reduced bromine concentration was observed near the surface, while peak integration indicated mass conservation; this may be explained by the preferential diffusion of PS to the surface, which has been observed by other researchers [11,24,39,50].

3. Results and discussion

As mentioned in Section 1, the PS/PBS system exhibits UCST behavior [14]. We have performed phase behavior studies on thin film blends of PS/PBS using scanning probe microscopy and SAXS [39] and measured the interaction parameter χ_{S-BrS} between brominated and non-brominated styrene segments as

$$\chi_{S-BrS} = -0.0833 + \frac{73.75}{T} \tag{2}$$

Here T is temperature reported in K. This expression assumes that χ_{S-BrS} is independent of composition, in agreement with previous studies [21]. The Flory–Huggins interaction parameter, χ, of a homopolymer, A, and a statistically random copolymer, A–B, is expressed as [4]

$$\chi = f^2 \chi_{AB} \tag{3}$$

Here f is the volume fraction of B repeat units in the random copolymer. Knowing the ratio of the molar volume of a styrene unit to that of a brominated styrene unit (0.862), f can be related to the extent of bromination, x, as [22]

$$f = \frac{x}{x + 0.862(1 - x)} \tag{4}$$

The mutual diffusion across the interface between two polymeric species can be described as a product of a kinetic term involving the tracer diffusion coefficients, degrees of polymerization, and compositions of the species, and a thermodynamic term that represents the driving force for mixing [51]. The thermodynamic term is given by $2\phi(1-\phi)(\chi_S - \chi)$ [9], where for our system, ϕ is the volume fraction of PBS copolymer and χ_S is the interaction parameter at the spinodal, given by

$$\chi_S = \tfrac{1}{2}\left(\frac{1}{N_{PS}(1-\phi)} + \frac{1}{N_{PBS}\phi}\right)$$

Here, N_{PS} and N_{PBS} are the respective degrees of polymerization. Thus, for values of $f > f_S$, the system becomes phase separated, with f_S given by

$$f_S = \sqrt{\frac{1}{2\left(-0.0833 + \frac{73.75}{T}\right)}\left(\frac{1}{N_{PS}(1-\phi)} + \frac{1}{N_{PBS}\phi}\right)} \tag{5}$$

The mutual diffusion coefficient can be expressed as

$$D_M = 2D_0\phi(1-\phi)(\chi_S - \chi) \tag{6}$$

Here D_0 is the kinetic term, a function of D_{PS} and D_{PBS}, the tracer diffusion coefficients of PS and PBS (and hence temperature and degree of polymerization) and their relative compositions. It is important to note that the tracer diffusion coefficient of the PBS copolymer is a function of the composition of the copolymer (f), but this dependence is expected to be weak for small f.

For the N-asymmetric systems, the kinetic term has been modeled using appropriate definitions of the segmental fluxes of the species across the interface, leading to the fast mode [30] and slow mode theories [27]. For D_0 modeled according to the slow mode theory, the mutual diffusion

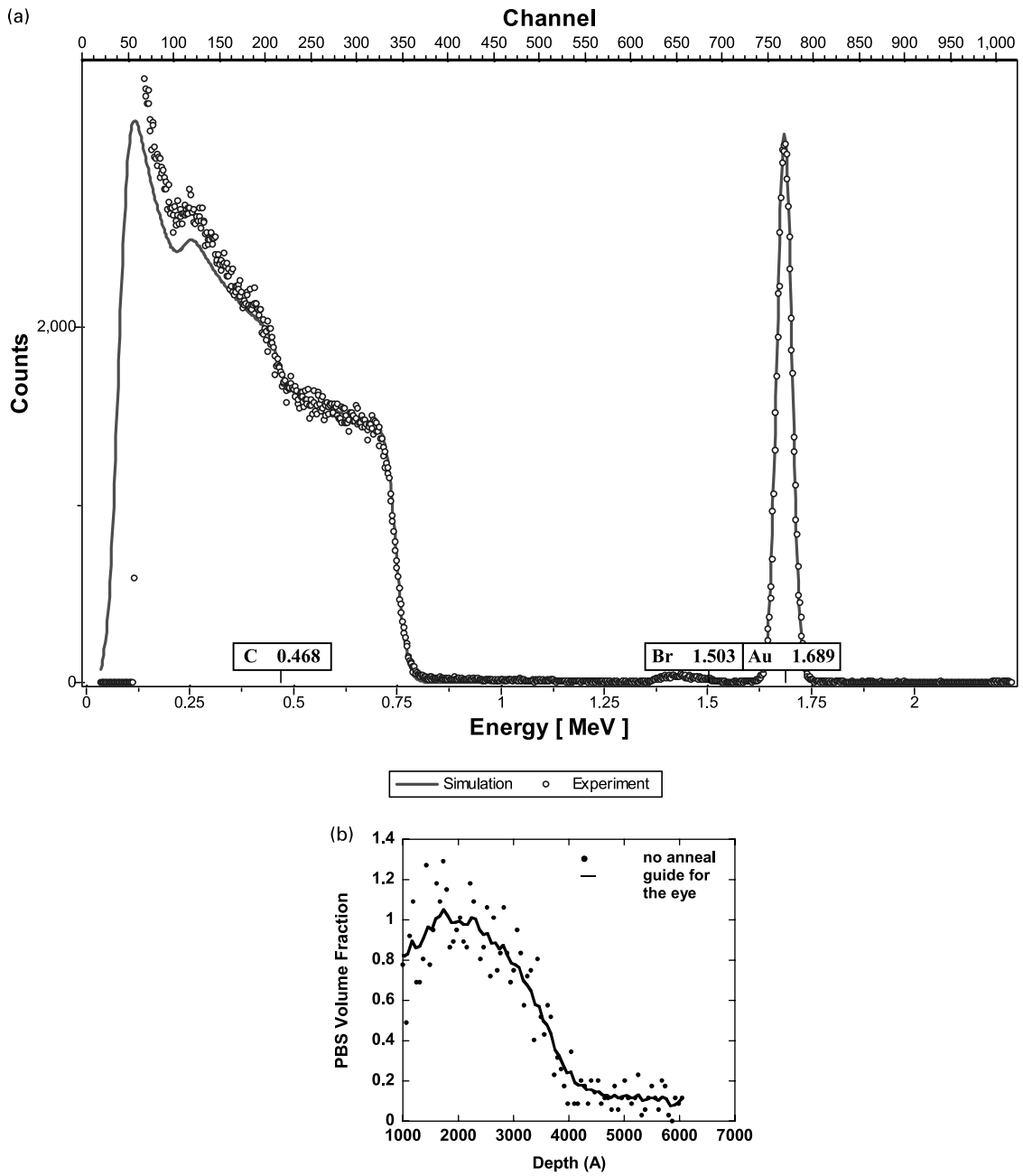

Fig. 1. Example of conversion from RBS yield versus channel/energy spectrum to PBS volume fraction versus depth profile. (a) Typical RBS spectrum is plotted in yield versus energy ($N_{PBS} = 7144, f = 0.04$, no anneal). This can be converted to PBS volume fraction versus depth by normalizing overall yield and converting energy to depth using the stopping range of ions in matter [44–46]. The peak corresponds to bromine and is representative of the PBS layer. (b) PBS volume fraction, ϕ, versus depth, z (Å), for an unannealed PS/PBS bilayer for $N_{PBS} = 7144$, $f = 0.04$. The thickness of this PBS layer is ~3100 Å.

coefficient, D_{MS}, is given by:

$$D_{MS} = \left(\frac{N_{PS}D_{PS}N_{PBS}D_{PBS}}{N_{PS}D_{PS}(1-\phi) + N_{PBS}D_{PBS}\phi}\right) \times \left(\frac{\phi}{N_{PS}} + \frac{1-\phi}{N_{PBS}} - 2\phi(1-\phi)\chi\right) \quad (7)$$

The fast mode theory expression for the mutual diffusion coefficient, D_{MF}, is given by:

$$D_{MF} = (\phi N_{PS}D_{PS} + (1-\phi)N_{PBS}D_{PBS}) \times \left(\frac{\phi}{N_{PS}} + \frac{(1-\phi)}{N_{PBS}} - 2\phi(1-\phi)\chi\right) \quad (8)$$

As mentioned before, the form of this equation leads to a mutual diffusion coefficient dominated by the faster moving component. It is instructive to note that the form of the

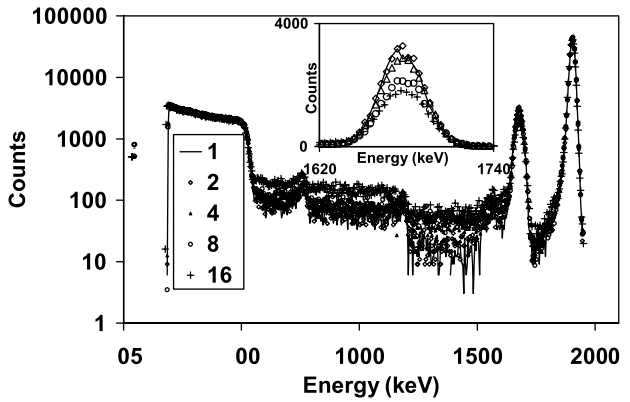

Fig. 2. Radiation damage study performed on an unannealed $N_{PS} = N_{PBS} = 1370$, $f = 0.55$ bilayer to determine the analysis time for which mass loss becomes significant. The symbols correspond to multiples of typical analysis time. The bromine peak is depicted in the inset; as shown, the sample can incur four times the usual dose before liberating HBr.

thermodynamic component of the mutual diffusion coefficient is common to both theories.

Jabbari and Peppas [35] have shown that the kinetic term of the mutual diffusion coefficient (Eq. (1)) contains a strongly composition-dependent monomeric friction coefficient for a polymer pair with dissimilar physical properties (e.g. PS/PVME). They obtain an expression for the blend monomeric friction factor as a function of molar specific volume, average number of repeat units between entanglements, and the average statistical length for the blend. The composition dependence of the monomeric friction factor arises due to the composition dependence of the various parameters that it depends on [35]. The PS/PBS system of interest is a polymer pair with similar physical properties for small values of f ($f < 0.25$) [21,41,52]. Another aspect of the PS/PBS system is that the glass transition temperatures of the two polymers differ by no more than 8 °C for $f < 0.25$ and all the annealing temperatures considered in this study are at least 35 °C above the T_gs. In contrast, the PS/PVME system is a polymer pair in which the T_gs differ by 128 °C [35]. Thus, in our analysis we have assumed that the monomeric friction coefficients for PS and PBS (for $f < 0.25$) are approximately equal and that this term does not have strong composition dependence since PS and PBS have similar properties. Thus, in the limit as $N_{PS} = N_{PBS}$ and $D_{PS} \approx D_{PBS}$, (good assumption for small f) the fast mode and slow mode expressions for D_M both reduce to the product of a constant kinetic term, D_0 ($\approx D_{PS} \approx D_{PBS}$), and the thermodynamic term, which remains unchanged.

Using this composition dependent D_M, profiles in the PS/PBS system can be fit to a mean-field interdiffusion model given by

$$\frac{\partial \phi}{\partial t} = \frac{\partial}{\partial z}\left(D_M(\phi)\frac{\partial \phi}{\partial z}\right) \tag{9}$$

Here z is the spatial position (depth), and t, time. This equation was solved numerically using an implicit finite difference method and compared to the RBS data using both D_{PS} and D_{PBS} as fitting parameters. All the N-asymmetric profiles were fit using the fast mode definition for the mutual diffusion coefficient (Eq. (8)).

Table 2
Mutual diffusion coefficient, D_M, for N-symmetric PS/PBS systems: D_M and $N\chi$ reported at 200 °C; D_M evaluated at $\phi = 0.5$

N	f	T range (°C)	$N\chi$	D_M (cm^2/s)
424	0	150–200	0	4.5×10^{-12}
	0.08		0.20	3.9×10^{-12}
	0.22		1.49	1.1×10^{-12}
	0.28		2.41	Binodal
	0.46		6.51	ND
	0.66		13.40	ND
1370	0	175–225	0	8.0×10^{-13}
	0.09		0.81	4.5×10^{-13}
	0.25		6.21	Binodal
	0.43		18.38	ND
	0.55		30.08	ND
4087	0	200–250	0	2.7×10^{-13}
	0.28		23.25	ND
	0.47		65.52	ND
	0.63		117.72	ND
7670	0		0	7.8×10^{-14}
7144	0.04	200–250	0.86	7.4×10^{-14}
	0.22		25.98	ND
	0.52		145.16	ND

3.1. Interdiffusion in N-symmetric PS/PBS systems

The characteristics of the N-symmetric PS/PBS system are shown in Table 2. At each of the annealing temperatures, the bilayers were annealed for various times from 15 to 180 min. As shown in Fig. 1, RBS spectra were converted to PBS volume fraction versus depth, (ϕ versus z), profiles. Fig. 3 shows ϕ versus normalized depth with a theoretical fit for PS/PBS for $N = 424$, $f = 0.08$ annealed for 15 min at 200 °C. Normalized depth is defined as z divided by the total thickness of the bilayer. Using Eq. (5), it can be verified that $f = 0.08$ is in the one-phase region for all temperatures considered in this study. Because the PS/PBS system is completely miscible, we see extensive interdiffusion after only 15 min. The D_0 value determined from this fit is 4.5×10^{-12} cm^2/s; this value is lower than the value for the tracer diffusion coefficient for PS (at the same N and T) reported in the literature, 25.4×10^{-12} cm^2/s [53]. However, this value is reasonable when compared to values obtained by Bruder and Brenn, which are reported to be a factor of 20 different than the value expected for similar systems [15,53]. One reason for the discrepancy in the work of Bruder and Brenn is that they use a constant mutual diffusion coefficient and an error function solution for the concentration profile. As mentioned earlier, increasing f decreases miscibility, which can be quantified by the term $N\chi$. The value of χ_S at $\phi = 0.5$ with $N_{PS} = N_{PBS} = N$ is given by $\chi_S = 2/N$, therefore, we use the criterion $N\chi < 2$

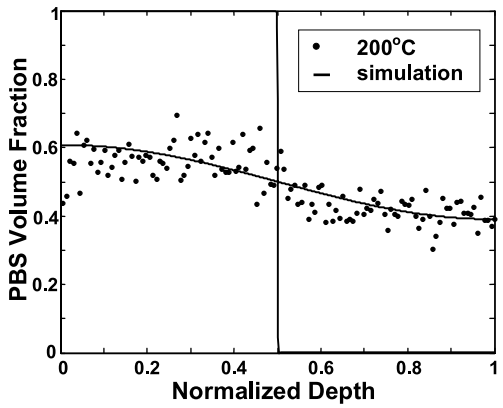

Fig. 3. PBS volume fraction, ϕ, versus normalized depth for PS/PBS bilayer ($N = 424, f = 0.08$) annealed at 200 °C with theoretical fit using fast mode theory, ● 15 m, — simulation.

to define completely miscible systems. The value of $N\chi$ is shown in Table 2 for each system. For $N = 424, f = 0.22$ at the annealing temperature of 200 °C, the system is still one phase, but approaching the phase boundary ($N\chi$ approaching 2) and would therefore be expected to have a decreased mutual diffusion coefficient. This dependence is reflected in the form of the thermodynamic term in Eq. (8); noting that the kinetic term D_0 should not change appreciably for small f, assuming D_{PBS} is a relatively weak function of copolymer composition for small f. Fig. 4 shows this effect for the case of $f = 0.22$; comparing this profile to Fig. 3, it is shown that for the same conditions of N and T, the interdiffusion in the system decreases due to decreased miscibility. It is important to note that, in Fig. 3, the initial PS and PBS layers have equal thickness and the equilibrium PBS volume fraction in the bilayer is 0.5. For the case in Fig. 4, the initial PBS layer is 40% of the total thickness of the bilayer, giving an equilibrium composition of 0.4. As discussed above, the D_0 value remains nearly unchanged ($D_0 = 4.0 \times 10^{-12} \times$ cm^2/s), while D_M decreases due to the higher value of f (Table 2).

At a still higher value of $f = 0.28$, the system reaches the phase boundary and interdiffuses only while layer

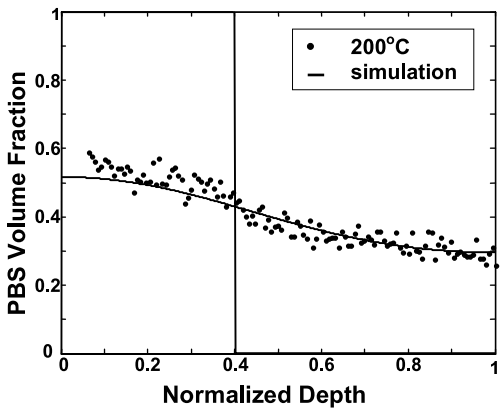

Fig. 4. PBS volume fraction, ϕ, versus normalized depth ($N = 424$, $f = 0.22$) annealed at 200 °C, ● 15 m, — simulation.

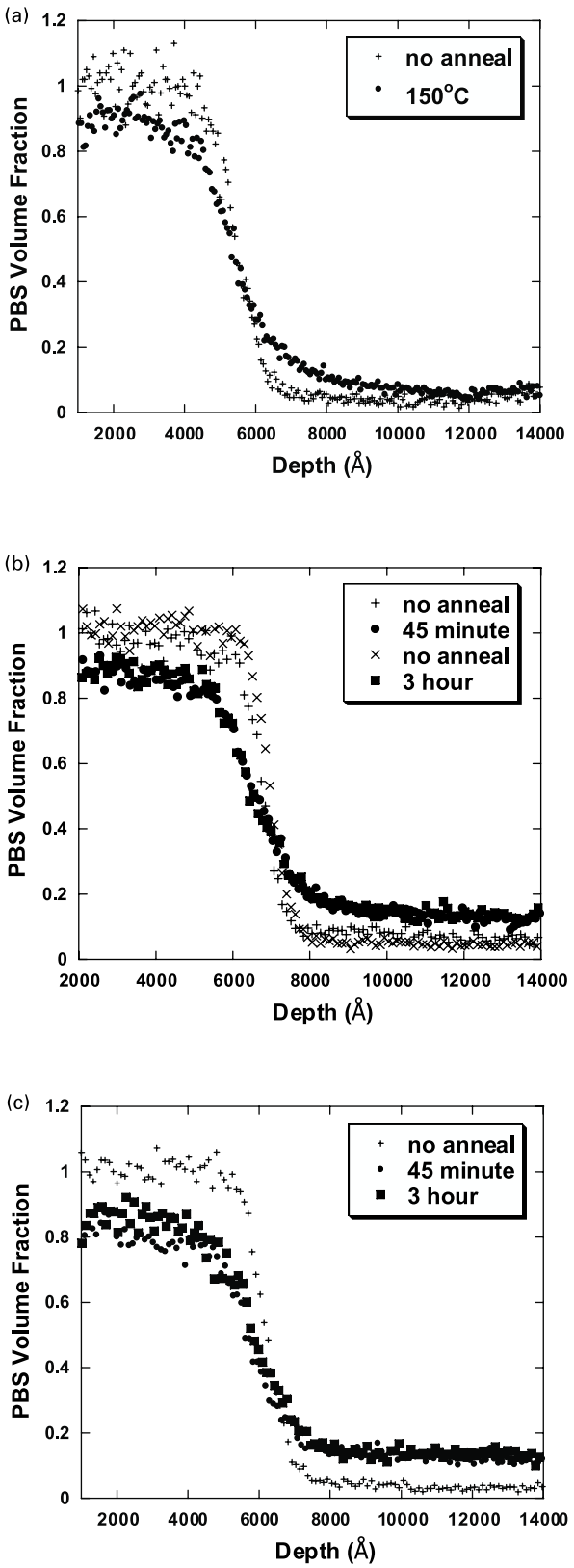

Fig. 5. PBS volume fraction versus depth profiles ($N = 424, f = 0.28$). (a) ϕ versus z, annealed at 150 °C, + no anneal, ● 3 h. (b) ϕ versus z, annealed at 175 °C, +, × no anneal, ● 45 min, ■ 3 h. (c) ϕ versus z, annealed at 200 °C, + no anneal, ● 45 min, ■ 3 h.

compositions remain in the one phase region; this interesting aspect is shown clearly in the RBS data. In Fig. 5, interdiffusion is observed at 150, 175, and 200 °C until the binodal compositions are reached. The phase diagram for PS/PBS ($N = 424$, $f = 0.28$) has been independently predicted using the χ parameter measured from SAXS and Flory–Huggins theory and is shown with the binodal compositions, calculated from the RBS data, in Fig. 6; all the phase diagrams shown in this paper have been predicted similarly. The binodal compositions determined from the RBS data are the average composition of the respective layers. There is very good agreement between the two independent measurements. This system is close to spinodal, thus, the term $(\chi - \chi_S)$ is small. It is known that the interfacial width, w, between two polymers is inversely proportional to the square root of $(\chi - \chi_S)$ [54], thus leading to measurable interfacial widths during the annealing times considered in this study. For the same system, increasing f to 0.46, the spinodal temperature well exceeds 200 °C and Fig. 7 shows the result when the interdiffusion in the system cannot be detected within the resolution of RBS, denoted 'ND'. It is instructive to note that the situations where no interdiffusion was detected show mass conservation and verify the success of the measures taken to alleviate radiation damage to PBS.

To quantify the effect of mobility in the system, PS/PBS of various N (424, 1370, 4087, 7144, and 7670) were used, as shown in Table 1. The profile for $N = 1370$, $f = 0.09$ at 225 °C is qualitatively similar to those for the miscible $N = 424$ cases. The value of D_0 from this fit is 3.5×10^{-12} cm^2/s, in good agreement with the value of D_{PS} from literature of 6.3×10^{-12} cm^2/s [53]. Investigating the effect of miscibility in this system, Fig. 8 shows the interdiffusion profiles for $N = 1370$, $f = 0.25$, for annealing temperatures of 175 and 200 °C. As in Fig. 5, this system reaches the phase boundary, thus giving rise to very steep interdiffusion profiles. For this reason, the mutual diffusion coefficient

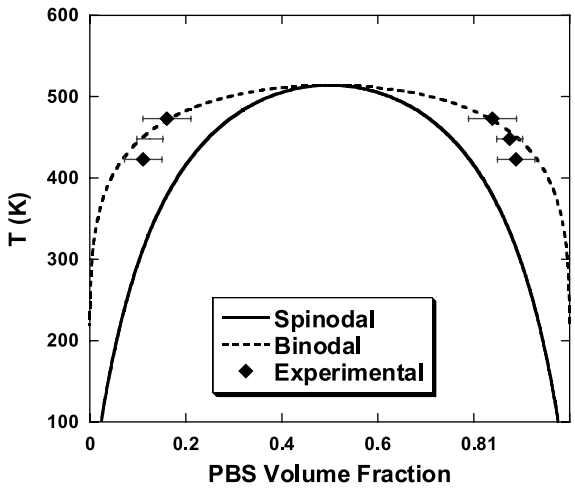

Fig. 6. Phase diagram for PS/PBS system ($N = 424$, $f = 0.28$) predicted from Flory–Huggins theory using χ from SAXS [39]. The ◆ points represent binodal layer compositions obtained from RBS (Fig. 5(a)–(c)).

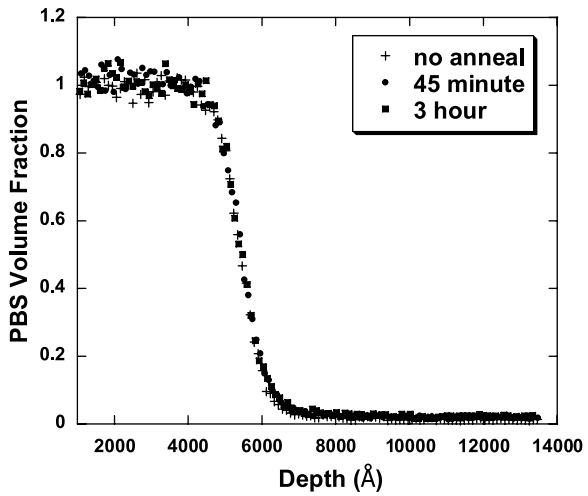

Fig. 7. PBS volume fraction, ϕ, versus depth, z, ($N = 424$, $f = 0.46$), annealed at 200 °C, + no anneal, ● 45 m, ■ 3 h.

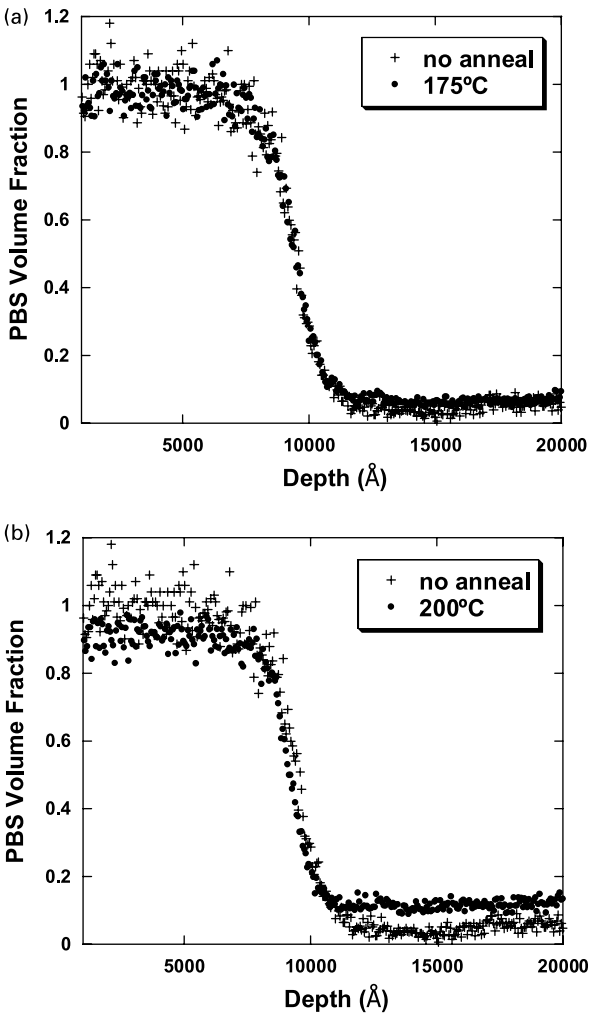

Fig. 8. PBS volume fraction versus depth profiles ($N = 1370$, $f = 0.25$). (a) ϕ versus z, annealed at 175 °C, + no anneal, ● 3 h. (b) ϕ versus z, annealed at 200 °C, + no anneal, ● 45 min.

cannot be accurately reported, but it is clear from the profiles that interdiffusion has taken place at the higher temperature. At 175 °C, interdiffusion cannot be detected within the resolution of RBS and is denoted 'ND'. At 200 °C, however, sufficient interdiffusion has taken place and the binodal compositions can be measured. The binodal compositions calculated from RBS are shown on the predicted phase diagram in Fig. 9; the agreement is fairly good. There is some variability due to the resolution (counts-wise) of the RBS instrument and due to the fact that this is very fast diffusion. In these cases, we expect layer compositions between the binodal and the spinodal.

When the degree of polymerization is again increased to $N = 4087$, all extents of bromination studied show no interdiffusion (data not shown). As N is further increased to 7670, no interdiffusion is observed when f exceeds 0.22, even at a temperature of 250 °C. There is visible interdiffusion for the miscible system with $f = 0.04$ at 200 and 225 °C, however, there is substantial scatter due to the very low extent of bromination (data not shown). The D_0 values calculated from these fits are 8.0×10^{-14} cm^2/s at 200 °C and 4.0×10^{-13} cm^2/s at 225 °C, consistent with literature values for D_{PS} of 7.8×10^{-14} and 2.0×10^{-13} cm^2/s at the respective temperatures [53]. Since the monomeric friction factor does not change appreciably for such small values of f, it is expected that D_{PBS} is very similar to the value of D_{PS} for the same N and T, therefore we expect D_0 to be a close approximation for both D_{PS} and D_{PBS} due to the very low extent of bromination, $f = 0.04$.

In summary, the values of the tracer diffusion coefficients D_{PS} and D_{PBS} determined from fitting the RBS data to PBS concentration profiles ranged from 10^{-14} to 10^{-12} cm^2/s. For immiscible systems, the RBS spectra for all the annealing temperatures and times remained unchanged, indicating that there is no interdiffusion and that mass is conserved. We note that the resolution of the RBS instrument limits detailed quantitative analysis and the comparisons of the various spectra and the fits provided are semi-quantitative. The D_0 values obtained from the RBS fits agree fairly well with the reptation prediction, $D_0 \sim N^{-2}$ (data not shown). The values of D_0 obtained from the fits were used to calculate the mutual diffusion coefficient, D_M. Table 2 summarizes the effect of both miscibility and mobility, as quantified by the term $N\chi$, on D_M for all values of T, f, and N studied; for given N, the system becomes more immiscible as the bromine content in the copolymer increases, and D_M decreases. When the phase boundary is crossed, interdiffusion is severely limited by the immiscibility in the system, this process has been referred to as 'uphill diffusion' and leads to spinodal decomposition. We have observed spinodal decomposition in thin film blends of PS/PBS for extents of bromination exceeding f_s using scanning probe microscopy as described elsewhere [39].

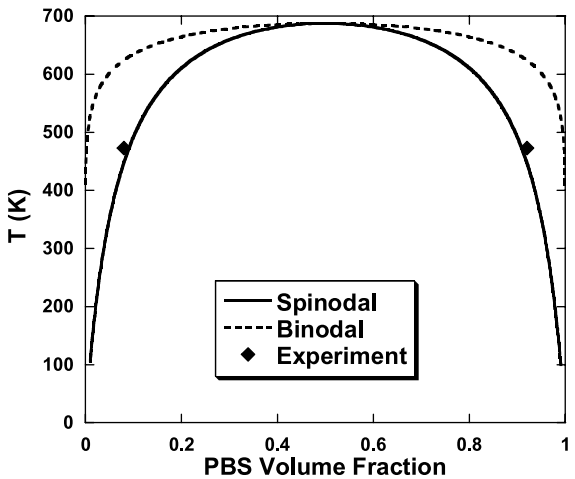

Fig. 9. Phase diagram for PS/PBS system ($N = 1370$, $f = 0.25$) predicted from Flory–Huggins theory using χ from SAXS [39]. The ◆ points represent binodal layer compositions obtained from RBS (a) and (b).

The results of the N-symmetric PS/PBS systems show the significant effect of the thermodynamic argument on the overall mutual diffusion coefficient. Our studies also show that decreased miscibility leads to a decreased mutual diffusion coefficient and that this thermodynamic effect dominates the kinetic effect argument (evidenced by a relatively unchanged D_0). This result has been observed by other researchers and termed thermodynamic slowing down [19,20,25,26].

3.2. Interdiffusion in N-asymmetric PS/PBS systems

All combinations of N, f, and T for the N-asymmetric samples studied are shown in Table 3. For N-asymmetric bilayers, we define a quantity $N^* = 2N_{PS}N_{PBS}/(N_{PS} + N_{PBS})$ that reduces to N when $N_{PS} = N_{PBS}$ and use the product $N^*\chi$ to quantify miscibility. The N-asymmetric data shows trends with degree of polymerization and extent of

Table 3
Mutual diffusion coefficient, D_M, for N-asymmetric PS/PBS systems: D_M and $N^*\chi$ reported at 200 °C; D_M evaluated at $\phi = 0.5$

N_{PS}	N_{PBS}	f	T range (°C)	$N^*\chi$	D_M (cm^2/s)
1370	424	0.08	175–225	0.30	1.9×10^{-12}
4087			200–225	0.36	1.5×10^{-12}
7670			200–225	0.37	1.2×10^{-12}
1370	424	0.22	175–225	2.27	Binodal
4087			200–225	2.70	Binodal
7670			200–225	2.82	Binodal
424	1370	0.09	175–225	0.38	1.8×10^{-12}
4087			200–250	1.21	2.0×10^{-13}
7670			200–250	1.37	1.1×10^{-13}
424	1370	0.25	175–225	2.94	Binodal
4087			200–250	9.31	ND
7670			200–250	10.54	ND
424	7144	0.04	200–225	0.09	1.4×10^{-12}
1370			200–250	0.27	3.0×10^{-13}
4087			200–250	0.60	1.1×10^{-13}
424	7144	0.22	200–225	2.81	Binodal
1370			200–250	8.08	ND
4087			200–250	18.26	ND

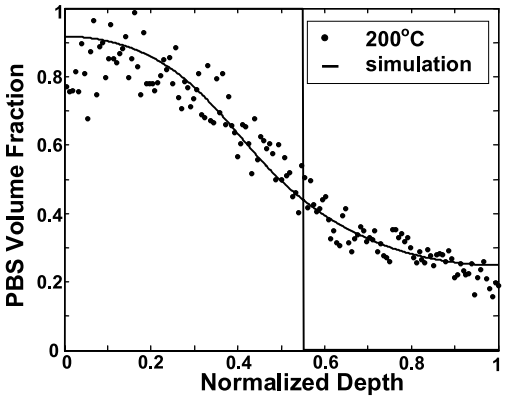

Fig. 10. Fast mode theory fit of N-asymmetric PS/PBS. PBS volume fraction, ϕ versus normalized depth profiles ($N_{PS} = 4087$, $N_{PBS} = 1370$, $f = 0.09$) annealed at 200 °C (● 30 min, — simulation).

bromination that are consistent with those observed for the N-symmetric system. Many binodal situations were encountered for the combinations of N_{PS}, N_{PBS}, f, and T chosen.

Using N-asymmetric bilayers, it is straightforward to show the validity of fast mode theory. For example, in Fig. 10, the system of $N_{PS} = 4087$, $N_{PBS} = 1370$, $f = 0.09$ at 200 °C, is fit with fast mode theory, using the definition for D_M given in Eq. (8). The values of D_{PS} and D_{PBS}, from the fast mode fit, are 2.7×10^{-13} and 8.0×10^{-13} cm^2/s, which are reasonable when compared to the values of $D_{PS} = 2.7 \times 10^{-13}$ and 2.4×10^{-12} cm^2/s for the same N, T, respectively, from literature [53]. The fit (not shown) with the slow mode theory (Eq. (7)) with the same values of D_{PS} and D_{PBS} as above gives a meaningless result since the slow mode theory imposes incompressibility on a system that is compressible. This result is consistent with previous observations [55], which reported validity of the compressible limit (i.e. fast-mode theory) for low molecular weights. The molecular weights used in our study are lower than the crossover molecular weight for PS reported by Feng et al. [55], thus supporting their conclusions.

The first N-asymmetric system of study combined various values of N_{PS} (1370, 4087, 7670) with $N_{PBS} = 424$ and $f = 0.08$. All combinations of $N_{PBS} = 424$ with the various N_{PS} at this f are miscible for the temperature range of study, and most resulted in flat interdiffusion profiles (indicating complete interdiffusion) after only 30 min with the exception of the case where $N_{PS} = 1370$, $T = 175$ °C. This profile with the fast mode fit is shown in Fig. 11(a). The values of D_{PS} and D_{PBS} obtained from this fit are 2.5×10^{-13} and 2.0×10^{-12} cm^2/s; these values are only slightly different from those obtained for the N-symmetric case, in agreement with expected values. Fig. 11(b) shows the situation when the degrees of polymerization of PS and PBS are reversed, i.e. $N_{PS} = 424$, $N_{PBS} = 1370$ with $f = 0.09$. The profiles show approximately the same extent of interdiffusion for the same annealing conditions (Fig. 11(a)). The values of D_{PS} and D_{PBS} from this fit are 2.0×10^{-12} and 2.5×10^{-13} cm^2/s, in agreement with the previous case.

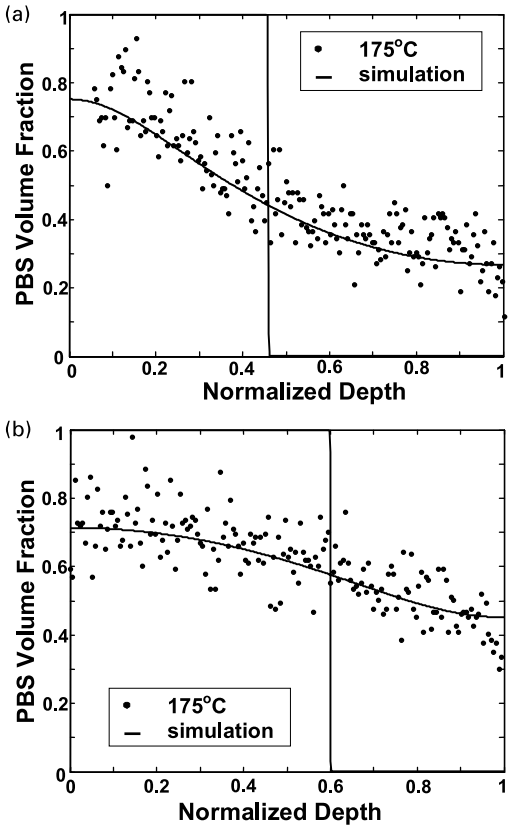

Fig. 11. PBS volume fraction, ϕ, versus normalized depth profiles for N-asymmetric PS/PBS systems. (a) $N_{PS} = 1370$, $N_{PBS} = 424$, $f = 0.08$, annealed at 175 °C, ● 30 min, — simulation. (b) $N_{PS} = 424$, $N_{PBS} = 1370$, $f = 0.09$, annealed at 175 °C, ● 30 min, — simulation.

The next system studied was $N_{PBS} = 424$, with increased extent of bromination ($f = 0.22$). In this case, all combinations with N_{PS} (as shown in Table 3) fall very near the phase boundary. Fig. 12 shows the result for $N_{PS} = 1370$ at three annealing temperatures; the composition of PBS in the PS layer at equilibrium is shown to increase with T, in agreement with UCST behavior. As the layers move toward compositions indicative of the phase boundary, it is also apparent that the interface is moving toward the faster diffusing component (as shown by the arrows) in conformity with fast mode theory. Another interesting aspect is that the composition of PBS in the PBS layer remains almost constant through a 50 °C change in temperature; this is consistent with the marked asymmetry of the phase diagram, Fig. 13, which clearly shows that the slope $dT/d\phi$ is much higher in the PBS-rich region.

Figs. 14 and 15 show another case where the PS and PBS layers are such that the degrees of polymerization are reversed, i.e. for a given value of f ($f = 0.22$), Fig. 14 shows the result when $N_{PBS}/N_{PS} = 0.055$, Fig. 15 shows the converse, $N_{PS}/N_{PBS} = 0.059$. Once again, the interface moves toward the faster diffusing species and the equilibrium compositions of the respective layers lie very near the phase boundary (the × marks are a guide for the eye). The N-asymmetric system of $N_{PS} = 4087$, $N_{PBS} = 7144$,

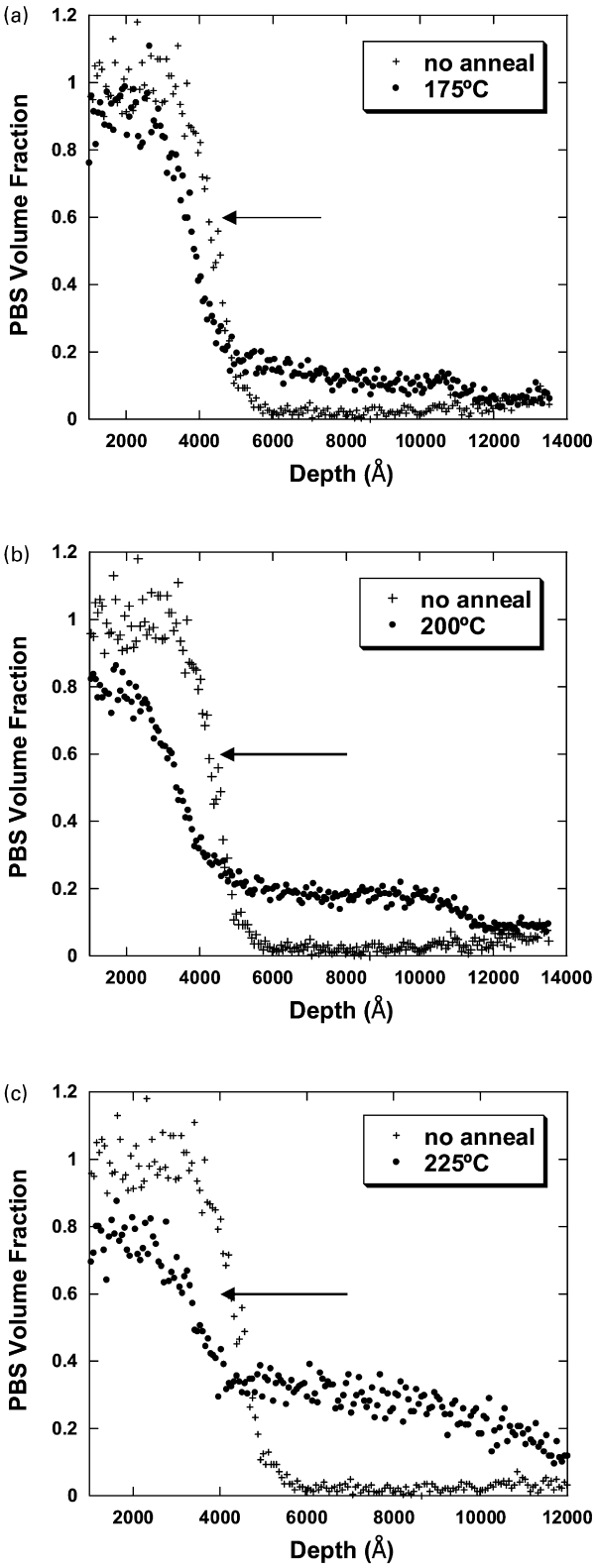

Fig. 12. PBS volume fraction, ϕ, versus normalized depth profiles for N-asymmetric PS/PBS bilayers near the binodal ($N_{PS} = 1370$, $N_{PBS} = 424$, $f = 0.22$). (a) ϕ versus z, annealed at 175 °C, + no anneal, ● 30 min. (b) ϕ versus z, annealed at 200 °C, + no anneal, ● 30 min. (c) ϕ versus z, annealed at 225 °C, + no anneal, ● 30 min.

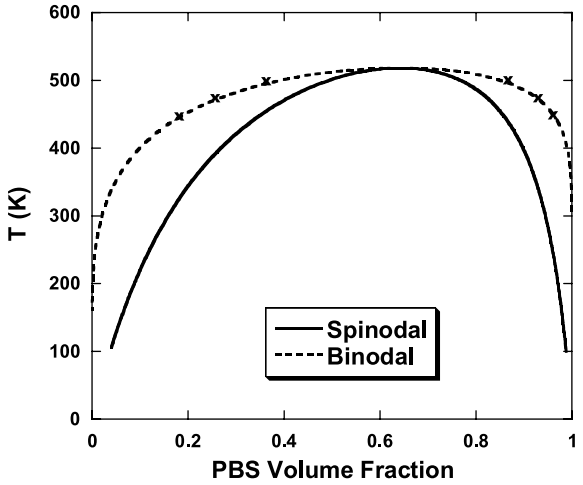

Fig. 13. Phase diagram for N-asymmetric PS/PBS system ($N_{PS} = 1370$, $N_{PBS} = 424, f = 0.22$) predicted from Flory–Huggins theory using χ from SAXS [39]. The × points are a guide for the eye to compare to binodal layer compositions from Fig. 12(a)–(c).

$f = 0.04$ is miscible at 225 °C and the value of D_{PBS} obtained from fitting this data to fast mode theory is $D_{PBS} = 3.6 \times 10^{-13}$ cm^2/s. This value is in excellent agreement with the value obtained for the N-symmetric case of $N = 7670, f = 0.04$ (see discussion on N-symmetric studies). This result supports the validity of using the fast mode theory approach to model both N-symmetric and N-asymmetric data.

The results of the N-asymmetric studies are summarized in Table 3 and show the effect of both the thermodynamic (miscibility) and kinetic (mobility) arguments on the overall mutual diffusion coefficient. An important consequence of the results of both the N-symmetric and N-asymmetric studies is that when χ is small and approaching χ_s, the interfacial width shows sufficient broadening to be measured. It has been shown that the fracture energy of an interface is directly proportional to the interfacial width [17]. Thus, by appropriately choosing χ (for example, by blending [27,56]), strategies can be developed to strengthen incompatible interfaces. For example, distributions in N and/or f can be advantageously used to promote interdiffusion at A/AB interfaces [57]. Hence, understanding miscibility-controlled interdiffusion phenomena might offer alternative approaches to reinforcement of polymer interfaces.

4. Conclusions

Interdiffusion behavior in the homopolymer/random copolymer system of PS/PBS was investigated using RBS. It was shown that interdiffusion is limited as the phase boundary is approached; layer compositions from the RBS data showed very good agreement with values from the binodal curve of the phase diagrams predicted using Flory–Huggins theory and a styrene–bromostyrene interaction

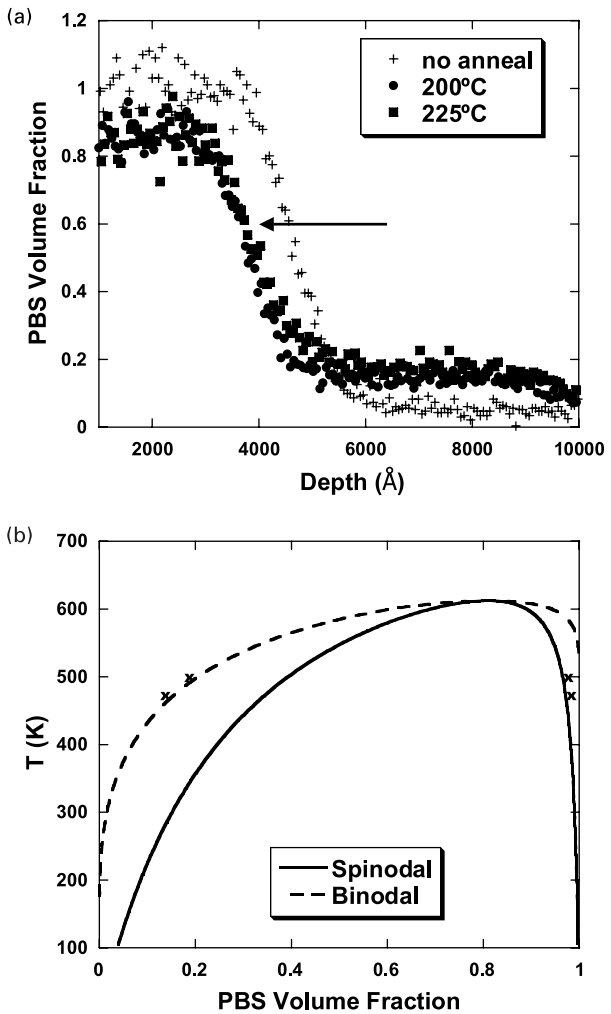

Fig. 14. PBS volume fraction, ϕ, versus depth profile (a) and phase diagram (b) for N-asymmetric PS/PBS bilayer near the binodal, $N_{PS} = 7670$, $N_{PBS} = 424$, $f = 0.22$. (a) ϕ versus z, + no anneal, ● 200 °C 30 min, ■ 225 °C 30 min. (b) Phase diagram for PS/PBS system ($N_{PS} = 7670$, $N_{PBS} = 424$, $f = 0.22$) [39].

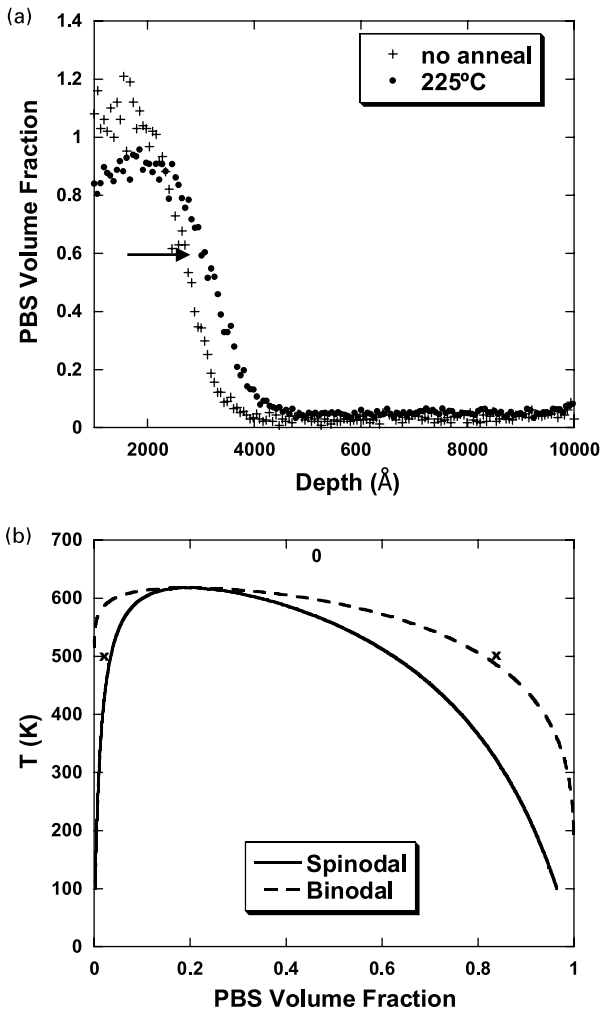

Fig. 15. PBS volume fraction, ϕ, versus depth profile (a) and phase diagram (b) for N-asymmetric PS/PBS bilayer near the binodal, $N_{PS} = 424$, $N_{PBS} = 7144$, $f = 0.22$. (a) ϕ versus z, + no anneal, ● 225 °C 30 min. (b) Phase diagram for PS/PBS system ($N_{PS} = 424$, $N_{PBS} = 7144$, $f = 0.22$) [39].

parameter measured using SAXS. For N-asymmetric interfaces, the mobility is dictated by the faster diffusing (lower N) component, consistent with fast mode theory, resulting in an interface that moved towards the faster diffusing component. It was also observed that equilibrium bilayer/interface conditions were consistent with the phase diagrams. Mutual diffusion coefficients were calculated for miscible systems by comparison of interdiffusion data from RBS spectra to a mean-field interdiffusion model based on fast mode theory. The mutual diffusion coefficient is shown to decrease with increasing N and x and increase with temperature. Semi-quantitative comparisons of the data with the fast mode theory at N-asymmetric PS/PBS interfaces yielded good agreement. The implications of this miscibility dependence of the interdiffusion behavior, based on both composition of the copolymer and degree of polymerization, are discussed in the context of strengthening homopolymer/random copolymer interfaces.

Acknowledgements

The authors thank Melissa Gregory and Carmen Fornarotto for assistance in synthesis and bilayer preparation and Robert Pfeffer and Wolf-Hartmut Schulte for assistance with the RBS studies. This work was supported by the National Science Foundation (CTS-0196338) and Union Carbide Corporation. This material is based upon work supported under a National Science Foundation Graduate Fellowship (to ELJ).

References

[1] Wool RP. Polymer interfaces structure and strength. New York: Hanser; 1995.
[2] Agrawal G, Wool RP, Dozier WD, Felcher GP, Zhou J, Pispas S, Mays JW, Russell TP. J Polym Sci, Part B: Polym Phys 1996;34:2919–40.
[3] Brochard F, de Gennes PG. Europhys Lett 1986;1(5):221–4.

[4] Bruder F, Brenn R, Stuhn B, Strobl GR. Macromolecules 1989;22: 4434–7.
[5] Composto RJ, Kramer EJ. J Mater Sci 1991;26:2815–22.
[6] de Gennes PG. Adv Colloid Interf Sci 1987;27:189–209.
[7] Composto RJ, Kramer EJ, White DM. Macromolecules 1988;21: 2580–8.
[8] Green P, Palmstrom CJ, Mayer JW, Kramer EJ. Macromolecules 1985;18:501–7.
[9] Jabbari E, Peppas NA. JMS Rev Macromol Chem Phys 1994;C34(2): 205–41.
[10] Jordan EA, Ball RC, Donald AM, Fetters LJ, Jones RAL, Klein J. Macromolecules 1988;21:235–9.
[11] Rafailovich MH, Sokolov J, Jones RAL, Krausch G, Klein J, Mills R. Europhys Lett 1988;5(7):657–62.
[12] Stamm M, Schubert DW. Annu Rev Mater Sci 1995;25:325–56.
[13] Whitlow SJ, Wool RP. Macromolecules 1989;22:2648–52.
[14] Kambour RP, Bendler JT, Bopp RC. Macromolecules 1983;16: 753–7.
[15] Bruder F, Brenn R. Macromolecules 1991;24:5552–7.
[16] Schnell R, Stamm M, Creton C. Macromolecules 1998;31:2284–92.
[17] Schnell R, Stamm M, Creton C. Macromolecules 1999;32(10): 3420–5.
[18] Bates FS, Wignall GD. Phys Rev Lett 1986;57(12):1429–32.
[19] Green P, Doyle BL. Phys Rev Lett 1986;57(19):2407–9.
[20] Green P, Doyle BL. Macromolecules 1987;20:2471–4.
[21] Koch T, Strobl GR. J Polym Sci, Part B: Polym Phys 1990;28: 343–53.
[22] Kambour RP, Bendler JT. Macromolecules 1986;19:2679–82.
[23] Guckenbiehl B, Stamm M, Springer T. Mater Res Soc Symp Proc 1993;280:275–80.
[24] Bruder F, Brenn R. Phys Rev Lett 1992;69(4):624–7.
[25] Losch A, Woermann D, Klein J. Macromolecules 1994;27:5713–5.
[26] Steiner U, Chaturvedi K, Zak O, Krausch G, Schatz G, Klein J. Mater Res Soc Symp Proc 1990;177:367–72. Macromol Liq.
[27] Brochard F, Jouffroy J, Levinson P. Macromolecules 1983;16: 1638–41.
[28] de Gennes PG. CRS Acad Sci, Ser 1981;2:1505–7.
[29] Jabbari E, Peppas NA. Polym Int 1995;38:65–9.
[30] Kramer EJ, Green P, Palmstrom CJ. Polymer 1984;25(4):473–80.
[31] Akcasu AZ. Polym Mater Sci Engng 1994;71:771.
[32] Akcasu AZ. Macromol Theory Simul 1997;6(4):679–702.
[33] Akcasu AZ, Naegele G, Klein R. Macromolecules 1995;28(19): 6680–3.
[34] Jabbari E, Peppas NA. Macromolecules 1993;26(9):2175–86.
[35] Jabbari E, Peppas NA. Polymer 1995;36(3):575–86.
[36] Meier H, Strobl GR. Macromolecules 1987;20:649–54.
[37] Sanchez IC. Physics of polymer surfaces and interfaces. Boston: Butterworth–Heinemann; 1992.
[38] Jabbari E, Peppas NA. J Mater Sci 1994;29:3969–78.
[39] Gorga RE, Jablonski EL, Thiyagarajan P, Seifert S, Narasimhan B. J Polym Sci, Part B: Polym Phys 2002;40:255–71.
[40] Kern W, Puotinen DA. RCA Rev 1970;31:187–206.
[41] Gorga RE, Narasimhan B. Submitted for publication.
[42] Kramer EJ. MRS Bull 1996;January:37–41.
[43] Lennard WN, McNorgan CP. http:/www.quarksimulation.com.
[44] Ziegler JF. The stopping ranges of ions in matter. Handbook of stopping cross sections for energetic ions in all elements, vol. 5. Oxford: Pergamon Press; 1980.
[45] Doolittle LR. Nucl Instr Meth 1985;9:344–51.
[46] Doolittle LR. Nucl Instr Meth 1986;15:227–31.
[47] Huttenbach S, Stamm M, Reiter G, Foster M. Langmuir 1991;7: 2438–42.
[48] Jones RAL, Richards RW. Polymers at surfaces and interfaces. Cambridge: Cambridge University Press; 1999.
[49] Feldman LC, Mayer JW. Fundamentals of surface and thin film analysis. New York: North Holland; 1986.
[50] Slep D, Asselta J, Rafailovich MH, Sokolov J, Winesett DA, Smith AP, Ade H, Strzhemechny Y, Schwarx SA, Sauer BB. Langmuir 1998;14:4860–4.
[51] Binder KJ. Chem Phys 1983;79(12):6387–409.
[52] Gorga RE, Narasimhan B. J Polym Sci, Part B: Polym Phys 2002;40: 2292–302.
[53] Tirrell M. Rubber Chem Technol 1984;57:523–56.
[54] Broseta D, Frederickson GH, Helfand E, Leibler L. Macromolecules 1990;23:132–9.
[55] Feng Y, Han CC, Takenaka M, Hashimoto T. Polymer 1992;33: 2729–39.
[56] Helfand E. Macromolecules 1992;25:1676–85.
[57] Benkoski JJ, Fredrickson GH, Kramer EJ. J Polym Sci, Part B: Polym Phys 2001;39:2363–77.